Journal of
Composites Science

MDPI

Article

Effect of Ethylene-1-Butene as a Compatibilizer for the Optimization of Wood Flour and Ground Tyre Rubber in Polypropylene Composites

Lefika Mosia, Mohau Justice Phiri *, Kathy Garde and Shanganyane Percy Hlangothi

Center for Rubber Science & Technology, Department of Chemistry, Nelson Mandela University, Gqeberha 6031, South Africa; lefikamosia@gmail.com (L.M.); kathy.garde@carst.co.za (K.G.); percy.hlangothi@mandela.ac.za (S.P.H.)
* Correspondence: mohaujphiri@gmail.com

Abstract: The use of waste materials to make eco-friendly wood-polymer composites has been explored by many researchers for academic and industrial purposes due to the low cost, biodegradability, and availability of waste wood flour. Polypropylene (PP)/ground tyre rubber (GTR)/wood flour (WF) composites were prepared using an internal batch mixer at a temperature of 165 °C for 8 min, and the samples were injection-moulded at 190 °C with a pressure of 6 MPa. The design of the experimental approach was used to determine and optimize the proportions of each component in the composites. The morphology of the untreated composites showed more voids and the agglomeration of fillers, namely WF and GTR, in the PP matrix. Fewer voids, as well as improved distribution, were observed in the compatibilized composites. The incorporation of ethylene-1-butene as a compatibilizer improved the thermal stability and elongation at the break of the composites. The addition of WF increased the elongation at break and decreased the tensile strength of the composites. Overall, the use of statistically designed experiments has aided in attaining the optimum formulations of the wood flour–polymer composites.

Keywords: wood flour–polymer composites; polypropylene; ground tyre rubber; recycling; design of experiments; thermo-mechanical; mechanical properties; morphological properties

Citation: Mosia, L.; Phiri, M.J.; Garde, K.; Hlangothi, S.P. Effect of Ethylene-1-Butene as a Compatibilizer for the Optimization of Wood Flour and Ground Tyre Rubber in Polypropylene Composites. *J. Compos. Sci.* **2022**, *6*, 220. https://doi.org/10.3390/jcs6080220

Academic Editor: Aleksander Hejna

Received: 14 June 2022
Accepted: 13 July 2022
Published: 29 July 2022

1. Introduction

In the last decade, researchers have developed ways to reduce the consumption of polymers and minimize the amount of dumped waste polymers in landfills [1–4]. Some of the strategies include the reuse of neat polymers more than once, blending the raw materials with recycled material, and recycling materials to produce secondary products [5,6]. Recycling reduces both the utilization of raw materials and the energy required for fabricating a new material, which leads to a reduction in air, water, and land pollution [7,8]. However, recycling has some drawbacks which need to be taken into consideration. The history of the recyclates must be well known to quantify the effect of fillers and additives in the composites, since most polymers are reinforced by different fillers and additives before reprocessing [9–11].

Wood flour (WF), ground tyre rubber (GTR), and other polymers have been utilized as reinforcements or fillers to improve the impact properties of polypropylene (PP), in particular [12–14]. Coupling agents, such as maleic anhydride and silanes, are often utilized to improve the compatibility between the PP matrix and various fillers [5,15,16]. The desired properties of the composites are achieved as a result of a good stress transfer and good interfacial adhesion between the polymer matrix and its components [17–19].

Several researchers have focused on producing polymer composites that are less costly and more environmentally friendly [20–24]. The properties of polymer/GTR/natural fibre composites have been extensively studied, and they have been found to have improved properties with a wide range of applications [25–27]. Factors that influence the morphology

of polymer-wood composites include particle size and the amount of WF [28–30]. Ndiaye et al. [3] reported that the dispersion of WF was better at a lower wood fibre content of 25 wt.%, but that as the loading increased to 50 wt.%, the blend formed aggregates which resulted in cavities and the failure of the polymer matrix to incorporate all the WF particles. The authors also reported that, after the addition of maleic anhydride grafted to PP as a coupling agent, the interfacial interaction adhesion of the PP/WF composites was improved and the debonding of large particles was prohibited. Thus, there were with fewer cavities compared to the blends without a coupling agent.

Ciro et al. [31] investigated the effect of GTR loading from 10–50 wt.% on the thermal stability of PP/GTR blends. It was reported that the thermal stability of all the blends was higher when compared to that of individually recycled PP and GTR. The blends showed a weight loss at around 310 °C, corresponding to the removal of a small number of compounds that have low molecular weights. The overall results showed that the thermal stability of blends decreased with the increase in the rubber content from 10–50 wt.%, due to the presence of additives, which initiated an early degradation process. Luo et al. [4] examined the effect of 60 and 80 mesh GTR on the mechanical properties of polypropylene/wood flour (PP/WF) composites. The authors observed an increase in tensile strength for all PP/WF/GTR composites after the addition of GTR from 5–15 wt.%. A significant increase was reported for the composites containing the least amount of GTR (5 wt.%), and there was improved impact strength of the PP/WF blends by 46%, due to the elastic nature of GTR material.

In this study, GTR and WF will be used to tailor the properties of PP in the presence and absence of ethylene-1-butene as a coupling agent. The main aim of this study is to investigate the influence of GTR and WF on the chemical, physical, thermal, and morphological properties of PP using a statistically designed simplex-centroid mixture design. It is, therefore, envisaged that findings from this study will also assist in the industrial development of waste materials into value-added products where mechanical strength is not a major requirement.

2. Materials and Methods

2.1. Materials and Chemicals

A homopolymer polypropylene with a density of 0.905 g/cm^3 and a melt flow index of 12 g/min measured at 230 °C with a load of 2.16 kg was supplied by the Sasol Company, South Africa. The waste WF with a particle size of 18 mesh size was supplied by a local furniture shop. The WF was obtained from a pine tree which contains ~50% cellulose, ~30% lignin and ~20% hemicellulose. The GTR, which has a particle size of 40 mesh, was obtained from truck and passenger car tyres, with a composition of styrene-butadiene rubber (SBR) and natural rubber (NR). Ethylene-1-butene (EB) was purchased from LG Chemicals. All the materials were used as received.

2.2. Mixing Approach and Injection Molding Procedures

Binary and ternary composites of PP, GTR, and WF were prepared using the proportions given by the data points, as shown by a circle dot, in Figure 1. The formulations were designed and optimized using a simplex-centroid mixture methodology approach. The materials were mixed in the Brabender internal mixer (Haake Thermo Scientific Polylab QC) at 165 °C with a speed of 50 rpm for 8 min. A three-step mixing procedure was used to achieve a good dispersion of fillers in the PP matrix. The PP was melted in the mixer for 4 min, the addition of GTR was followed by WF in the last 4 min, and the samples were injection moulded. To evaluate the effect of the compatibilizer, some composites were prepared with ethylene-1-butene as a compatibilizer, as shown in Table 1. When PP was the main component, its content was varied in the rage of 60–86 wt.%, while amounts of GTR and WF were limited between 0–40 wt.% in the composites.

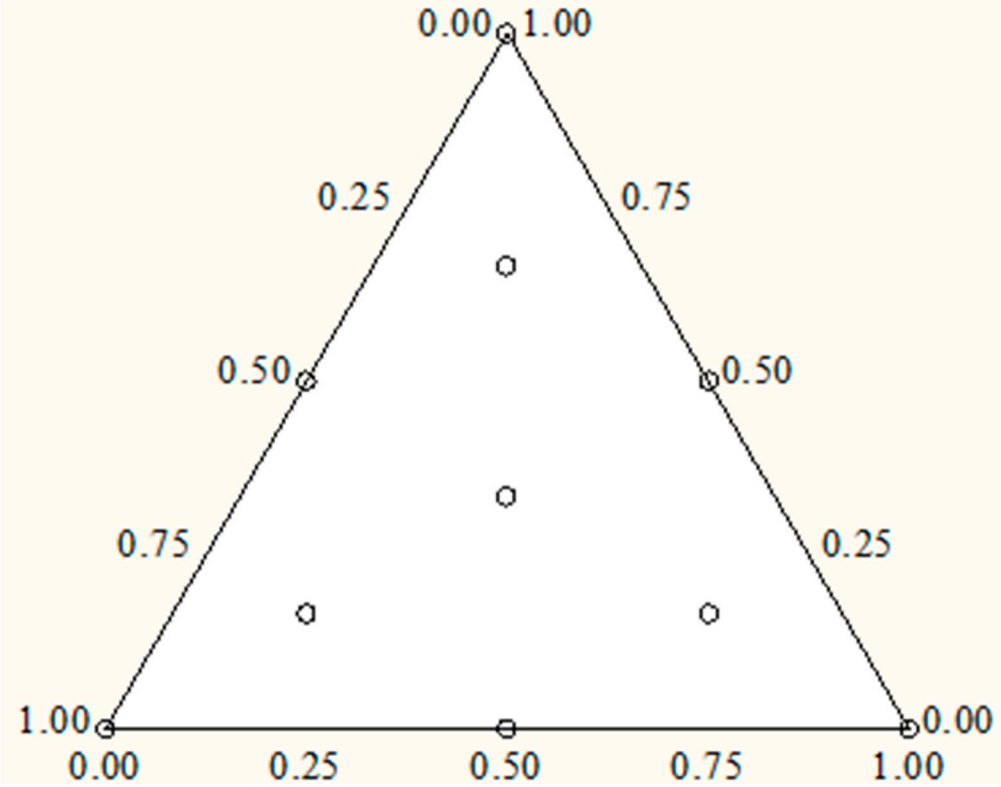

Figure 1. The experimental formulations, shown as a circle dot, for the binary and ternary blends of the PP/WF/GTR samples designed by a simple-centroid mixture methodology approach.

Table 1. The melting behaviour of the composites with and without EB as a compatibilizer.

Sample #	PP (%)	GTR (%)	WF (%)	Absence of EB		Presence of EB	
				T_m (°C)	ΔH_m (J/g)	T_m (°C)	ΔH_m (J/g)
1	60	40	0	163.7	57.6	162.5	56.6
2	60	0	40	163.6	68.6	163.4	52.9
3	66	27	7	162.0	87.1	156.8	62.8
4	66	7	27	164.2	72.5	164.1	60.8
5	86	7	7	162.3	90.0	166.0	67.0

An injection moulding machine (ARBURG 221-55-250) was used to obtain the specimens for further characterization. Injection moulding zones were programmed as follows: melt temperature at the feed zone at 170 °C, the centre at 180 °C, and the front zone and the nozzle at 190 °C. The nozzle was operated at holding and injection pressures of 40 and 60 MPa, respectively, with a speed of 2 mm/s. The obtained injection moulded specimens were further characterized by various analytical techniques.

2.3. Thermal Analysis of the Composites

A TA Instruments' Discover Series DSC was used for the thermal analysis of the composites. The sample with a mass range of 3.0–5.0 mg was analysed under a nitrogen atmosphere at a flow rate of 50 mL/min. The first and second heating and first cooling runs were performed at a temperature range of 20–180 °C at a heating rate of 10 °C/min. The first cooling and second heating measurements were used for data analysis. The first heating was performed to remove the thermal history and to eliminate any impurities within the sample.

A Q600 Discovery Series, high-resolution thermogravimetric analyser (Hi-Res™-TGA) was used to study the thermal degradation behaviour of the composites. A sample with

a mass of ~15 mg was heated from 20–600 °C under nitrogen gas with a flow rate of 50 mL/min at a heating rate of 10 °C/min.

2.4. Water-Resistance Analysis of the Composites

The water-resistance properties of the cured samples were measured using absorption experiments by following the ASTM D 570 specifications [32]. Before analysis, the samples with a width of 6.18–6.23 mm, thickness of 4.06–4.20 mm, and a diameter of 9.34–0.51 mm were placed in an oven for 48 h at 50 °C to remove any moisture. The dried samples were weighed and immersed in water for 6 days at ambient temperature. During the 6 days, soaked composites were taken out after every 12 h, tapped gently using a paper towel, and then weighed. Water absorption percentages (WA%) of the samples were calculated based on the following Equation (1), where M_i and M_f are the initial and final masses, respectively:

$$WA\% = ((M_f - M_i)/M_i) \times 100 \quad (1)$$

2.5. Mechanical Analysis of the Composites

Tensile strength and elongation at break properties of the composites were measured using a Tensometer, ENT 6005, with a crosshead speed of 500 mm/min. Dog-boned shaped samples with a length of 104.98 mm, a width of 10.22 mm, and a thickness of 4.98 mm were injection moulded using the ARBURG 221-55-250. The ASTM D 638 test method was followed for tensile testing [5]. The gauge length of 25 mm was used for the analysis, and three specimens were tested per composite.

2.6. Dynamic Mechanical Analysis of the Composites

The dynamical mechanical properties of the composites were measured using a dynamic mechanical analyser (DMA), model Q800. The sinusoidal stress was applied on the rectangular sample with a length of 17.88 mm, width of 6.05–6.88 mm, and a thickness of 4.10–4.20 mm, and the resulting strain was measured. The single cantilever mode of deformation was used with a multi-strain mode. At the start of the analysis, the sample was kept isothermal for 1 min and, thereafter, it was heated from −70 °C to 120 °C at a heating rate of 5 °C/min under the nitrogen atmosphere. The analysis was performed with the amplitude and frequency of 10 μm and 1 Hz, respectively.

2.7. Morphological Analysis of the Composites

The morphological properties of the composites were studied using a Joel JSM-IT100 scanning electron microscope (SEM). The samples were taken from fractured tensile specimens. The instrument was operated at an acceleration voltage between 10 and 15 kV. The samples were coated with gold before the analyses.

3. Results and Discussion

3.1. Thermal Properties of the PP/GTR/WF Composites

The results of the melting behaviour of composites are presented in Table 1. The melting temperature of the neat PP was observed at 161.2 °C, and the highest melting point that was reached for the untreated composites was 164.2 °C for the PP/GTR/WF composite, which was Sample 4. The melting temperature of the composites increased with the addition of GTR and WF for both the binary and ternary composites, but a significant increase was observed in the binary composites having only PP and GTR. The composites with more WF than GTR showed increased melting temperature, since WF can act as a nucleating agent, which can increase the crystallites' size and result in higher melting temperature values. The addition of a compatibilizer decreased the melting temperature of all the composites, possibly because the compatibilizer could have hindered the molecular movement of PP by interacting with WF and GTR. Furthermore, the decrease could have been a result of introduced flexibility from the elastomeric nature of the compatibilizer

(ethylene-1-butene) and resulted in reduced crystallites size. The melting enthalpy is related to the total crystallinity of a material. The melting enthalpies of the ternary composites as depicted in Table 1 were observed to be higher than those of the binary composites, and the presence of the compatibilizer decreased the melting enthalpies of all composites.

Figure 2 shows the TGA results of the untreated and compatibilized PP/GTR/WF composites. The untreated composites result, as depicted in Figure 2A, showed that Sample 5 has a single degradation step, which indicate good interaction among the PP matrix and GTR/WF components. The increase in the amount of either GTR or WF to 27 wt.% resulted in the composites exhibiting two degradation steps, where the first step is due to GTR and possibly the degradation of WF, depending on their amounts, and the second step can be attributed to the degradation of the PP matrix. Sample 5 also showed higher miscibility due to the PP component in the composites, and its thermal stability was lower than that of Samples 3 and 4. The composite containing more GTR than WF, Sample 3, showed higher thermal stability than the composite containing more WF than GTR, Sample 4.

The TGA curves of EB compatibilized PP/GTR/WF composites are shown in Figure 2B. The thermal stability of Sample 1 and Sample 4 decreased after the addition of the compatibilizer, whereas there was improved wetting between the PP matrix and GTR particles as Sample 1 changed from heterogeneity to homogeneity. On the other hand, the thermal stability of Sample 5 decreased after the addition of the compatibilizer due to debonding amongst the components of the composites. This decrease might be due to the preference of the compatibilizer for one component in the composite. Several authors have suggested that a compatibilizer can favour one component over the other, which, thus, causes good interfacial bonding between one filler and the matrix while excluding the other filler.

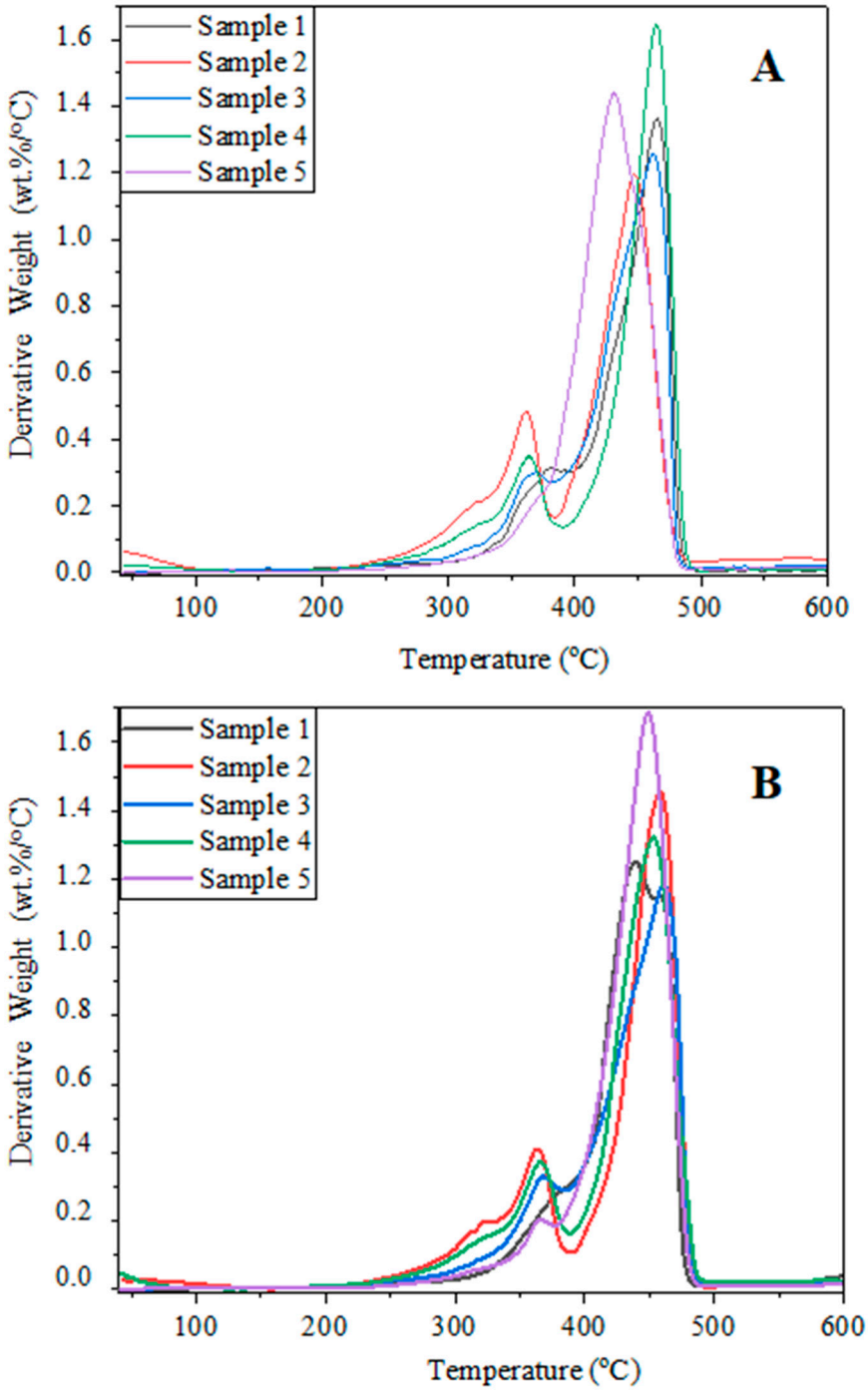

Figure 2. Thermogravimetric analysis results of the untreated (**A**) and EB compatibilized (**B**) PP/GTR/WF composites.

3.2. Mechanical Properties of the PP/GTR/WF Composites

The tensile properties of untreated and EB compatibilized PP/GTR/WF composites are shown in Figure 3. The maximum tensile strength for untreated composites was ≥34 MPa, as in Figure 3A, while that of the EB compatibilized composites was observed at ~26 MPa, as in Figure 3B. The neat PP showed the highest tensile strength of all the composites, irrespective of whether it was untreated or compatibilized with EB. The tensile strength of the composites decreased upon the addition of GTR and WF; this was more evident for the composites that contain a higher amount of GTR in both untreated and EB compatibilized composites. The decrease with the addition of GTR was due to the

low mechanical properties of GTR and poor adhesion between the PP matrix and GTR particles. There was a decrease in the tensile strength of the composites as the WF content was increased due to poor interfacial adhesion caused by aggregates of WF within the PP matrix. The compatibilizer did not cause any significant positive change to the tensile strength of the composites; instead, it weakened the strength of the composites.

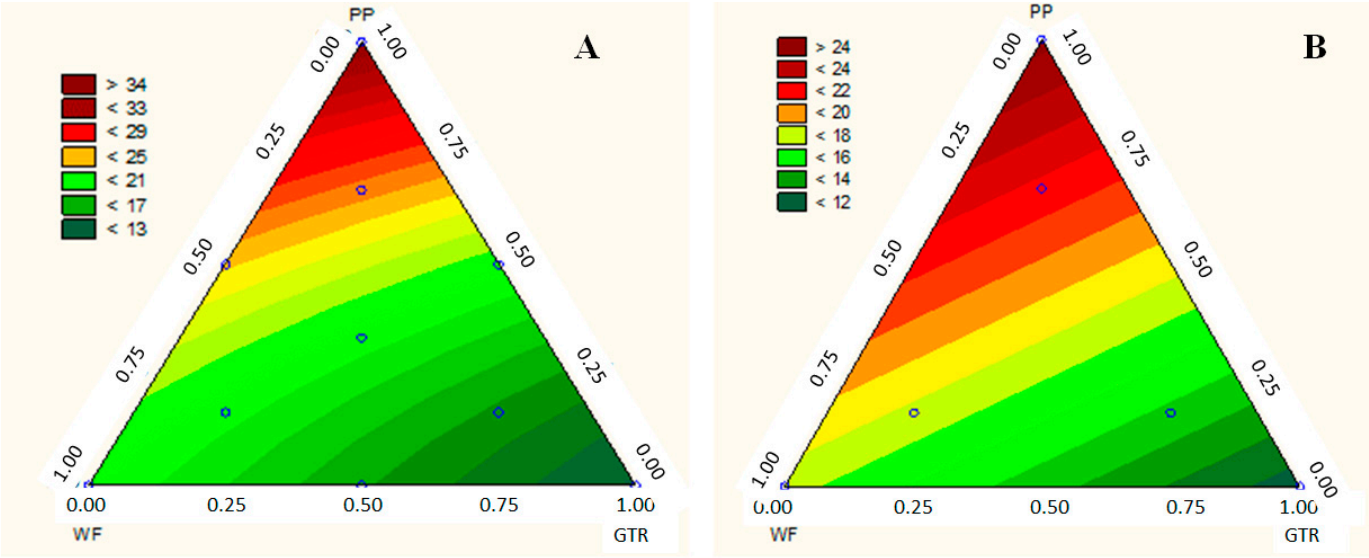

Figure 3. Tensile strength results of the untreated (**A**) and EB compatibilized (**B**) PP/GTR/WF composites.

The tensile strength results of composites compatibilized with EB demonstrated a linear model, as shown by straight lines, thus suggesting that there were no interactions of the components observed in the composites, as in Figure 3B. For untreated composites, there were interactions among the components of the composites, as shown by the contour lines in Figure 3A. Figure 4 shows the Pareto chart for the interaction among the components of the untreated and EB compatibilized composites. The observed interaction among the components in the untreated composites meant that each component had either a positive or negative effect on the tensile strength of the composites. The significance of each variable was determined by the *p*-value greater than 0.05, and PP was found to have the greatest positive influence on the tensile strength for both untreated and EB compatibilized composites, as presented in Figure 4A,B, respectively. Figure 4A also showed a statistically significant interaction between PP and GTR, and between PP and WF components, which resulted in a decrease in the tensile strength of composites. Based on the magnitude of both interactions in Figure 4A, GTR has a more negative effect than WF on the tensile strength of the composites. Lastly, WF on its own contributed positively towards the overall tensile strength of the composites.

Figure 5 shows the elongation at break for the untreated and EB compatibilized PP/GTR/WF composites. It can be seen in Figure 5A that the addition of GTR significantly improved the elongation at break of the composites, more so than the addition of WF due to the elastomeric nature of GTR. The maximum elongation at break observed was $\geq$12% and $\geq$14% for untreated and EB compatibilized composites, respectively. The results show that a compatibilizer increased the elongation at break of the composites due to the elastomeric nature of EB. The statistically significant interaction that occurred between PP and GTR was found to have a negative effect on the elongation at break. Moreover, there was a decrease in the elongation at break of the composites with an increase in WF content, attributable to high stiffness of WF, as well as poor interfacial adhesion between the PP matrix and the fibre particles.

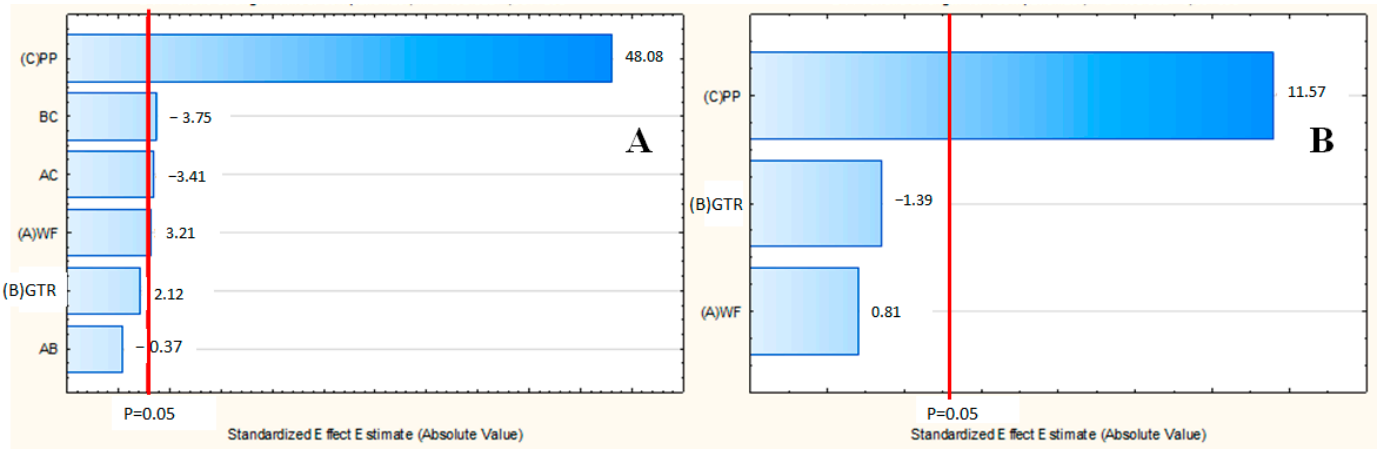

Figure 4. Tensile strength results of the untreated (**A**) and EB compatibilized (**B**) PP/GTR/WF composites showing the effect of interactions among the components.

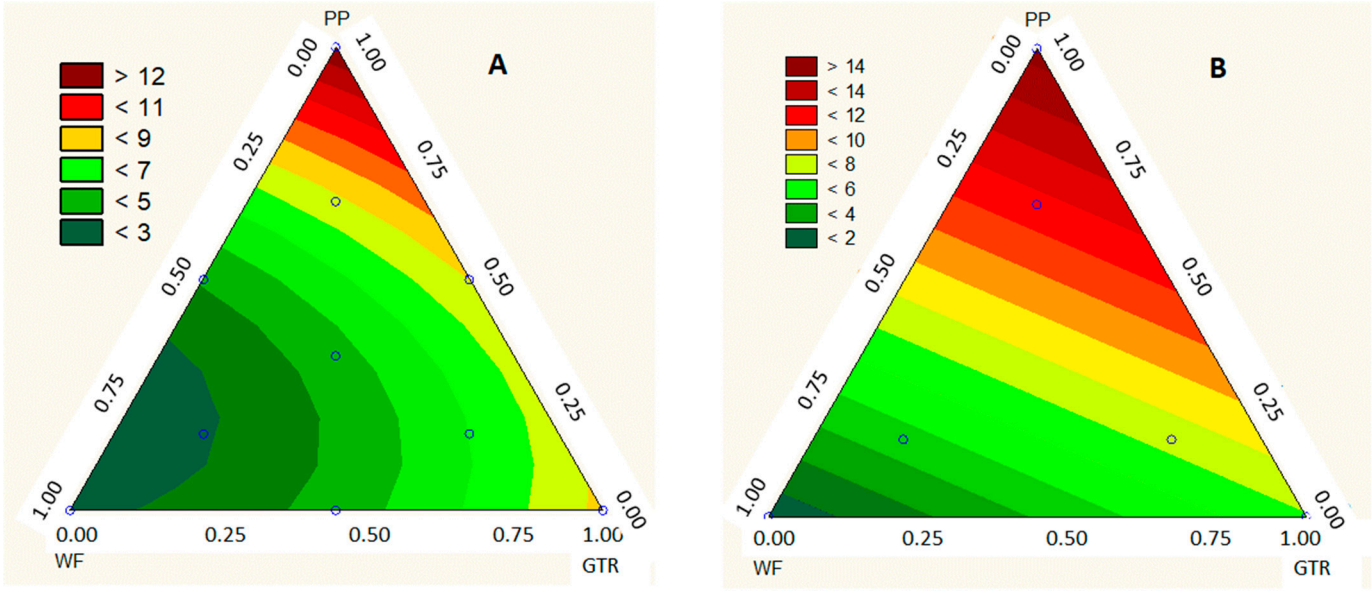

Figure 5. Elongation at break results of the untreated (**A**) and EB compatibilized (**B**) PP/GTR/WF composites.

3.3. Dynamic Mechanical Properties of the PP/GTR/WF Composites

The effect of the compatibilizer on the dynamical properties of the composites was studied using DMA. The results of the storage modulus for the untreated and compatibilized PP/GTR/WF composites are depicted in Figure 6. The untreated composites with high amounts of WF, namely Samples 2 and 4, show increased storage modulus among the samples, as displayed in Figure 6A. The WF has particles which are brittle and rigid, which has resulted in increased storage modulus, and the storage modulus of the material is related to its stiffness or rigidity [29]. Upon the addition of the compatibilizer, the maximum storage modulus of the composites drops significantly, except for Sample 2 with the highest amount of WF, as shown in Figure 6B. The assumption is that the EB compatibilizer acts as a binder within the composites to decrease their stiffness, and results in improved processing conditions in terms of rheological behaviour.

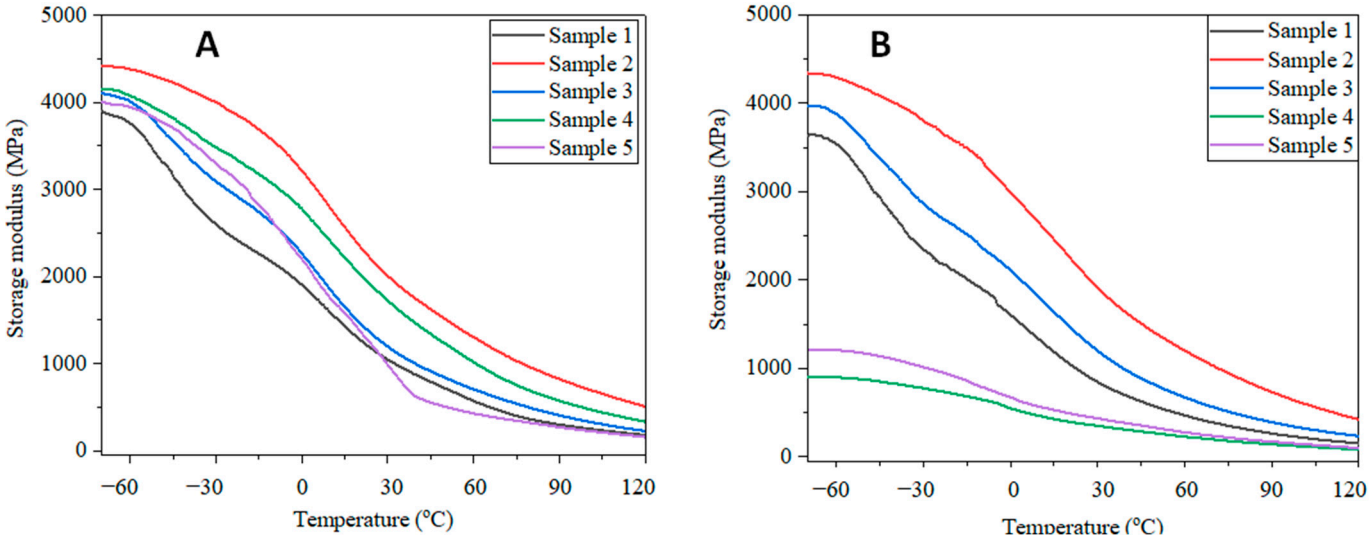

Figure 6. Storage modulus results of the untreated (**A**) and EB compatibilized (**B**) PP/GTR/WF composites.

Figure 7 shows the tan delta results of the untreated and compatibilized PP/GTR/WF composites. The tan delta is related to the impact properties of the material, since it is measured at the glass transition temperature, Tg. There are two sets of tan delta peaks observed in Figure 7A,B. The first set of peaks at ~−45 °C is assigned to the rubber material in GTR [33], as it is confirmed by Samples 1 and 3 that these have a higher amount of GTR, and the second set of peaks at ~5 °C is due to the glass transition behaviour of the PP matrix. It is observed that in the composites with a high amount of WF, as displayed in Figure 7A, tan delta values shifted to higher temperatures, indicating that WF particles disrupted the chain mobility in the PP matrix, thus resulting in lower damping behaviour of the composites [29,34]. There is a significant decrease in the tan delta of Sample 5 after the addition of a compatibilizer, as shown in Figure 7B. This could be due to the elastomeric nature of the EB compatibilizer, and it has indirectly introduced flexibility and initiated chain mobility within the composites. The tan delta of Sample 4 decreased drastically after the addition of the compatibilizer, reflecting that EB hindered the formation of WF agglomeration, but it has induced the entanglement of WF particles within the PP matrix.

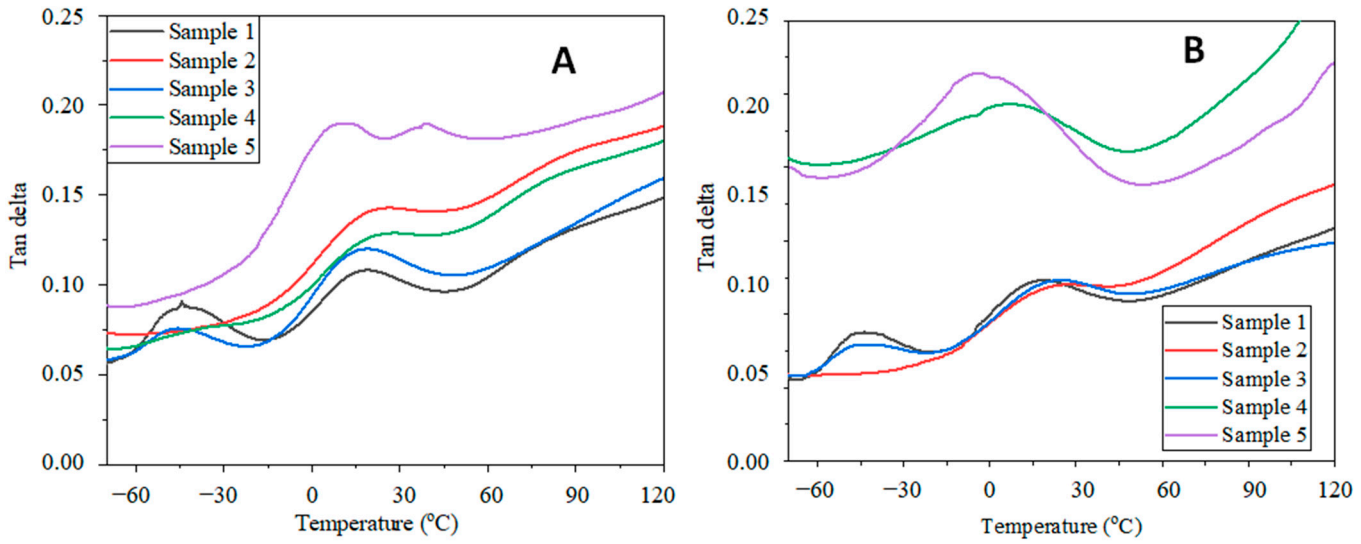

Figure 7. Tan delta results of the untreated (**A**) and EB compatibilized (**B**) PP/GTR/WF composites.

3.4. Water Resistance Properties of the PP/GTR/WF Composites

The results of untreated and EB compatibilized PP/GTR/WF composites are shown in Figure 8, and there is a similar trend for all the composites with relatively low WF content. The increase in WF content increased the absorption of water in the composites, since wood particles consists of hydroxyl groups which have a strong affinity to water, and there could also be a weak interfacial adhesion between PP matric and WF particles that caused voids in the composites. The addition of a compatibilizer decreased the water uptake for all the binary and ternary composites, especially the ones containing GTR. The decreased water uptake might be due to a better interfacial adhesion between the PP matrix and GTR particles. In addition, some of the cavities present in untreated composites could be blocked by the compatibilizer, thus, restricting water from entering the composites.

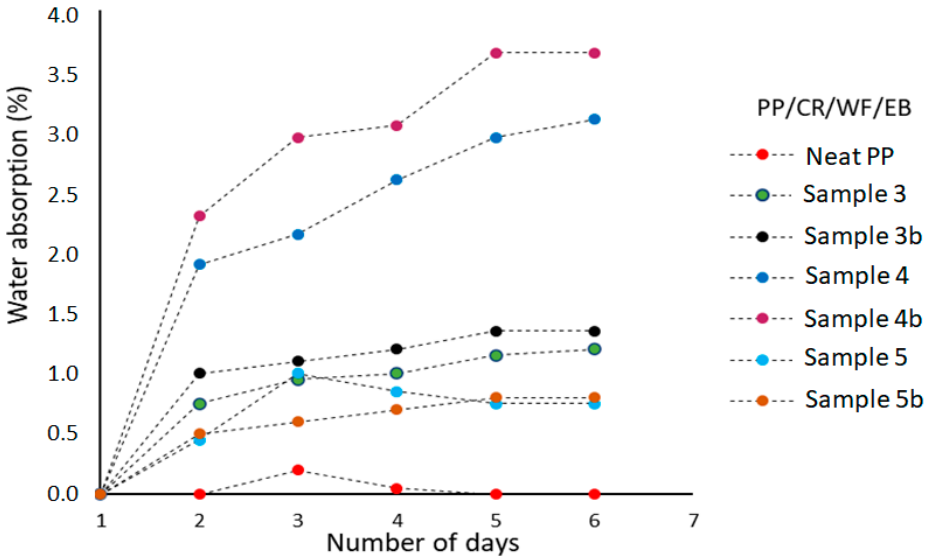

Figure 8. The percentages of water absorption for the PP/GTR/WF composites. Here, #b denotes samples prepared in the presence compatibilizer.

3.5. Morphological Properties of the PP/GTR/WF Composites

The results of the morphological analyses on the untreated and EB compatibilized PP/GTR/WF composites are presented in Figure 9. The SEM images of the EB compatibilized binary composite, Sample 1b, is shown in Figure 9A, and it can be seen that the GTR is well distributed and dispersed in the PP matrix, while a few small voids are present in the composites. This result is similar to the tensile strength results that indicated that the compatibilizer did not significantly enhance the interfacial adhesion between the PP matrix and GTR particles. Sample 2b shows a rough and uniform surface, and it can be seen in this composite that the PP encapsulated the WF particles, even though a small portion of WF particles were not fully covered due to the high wood flour content of 40 wt.%. This composite showed improved interfacial bonding between the WF particles and the PP matrix, as there were fewer gaps observed due to the EB compatibilizer effect.

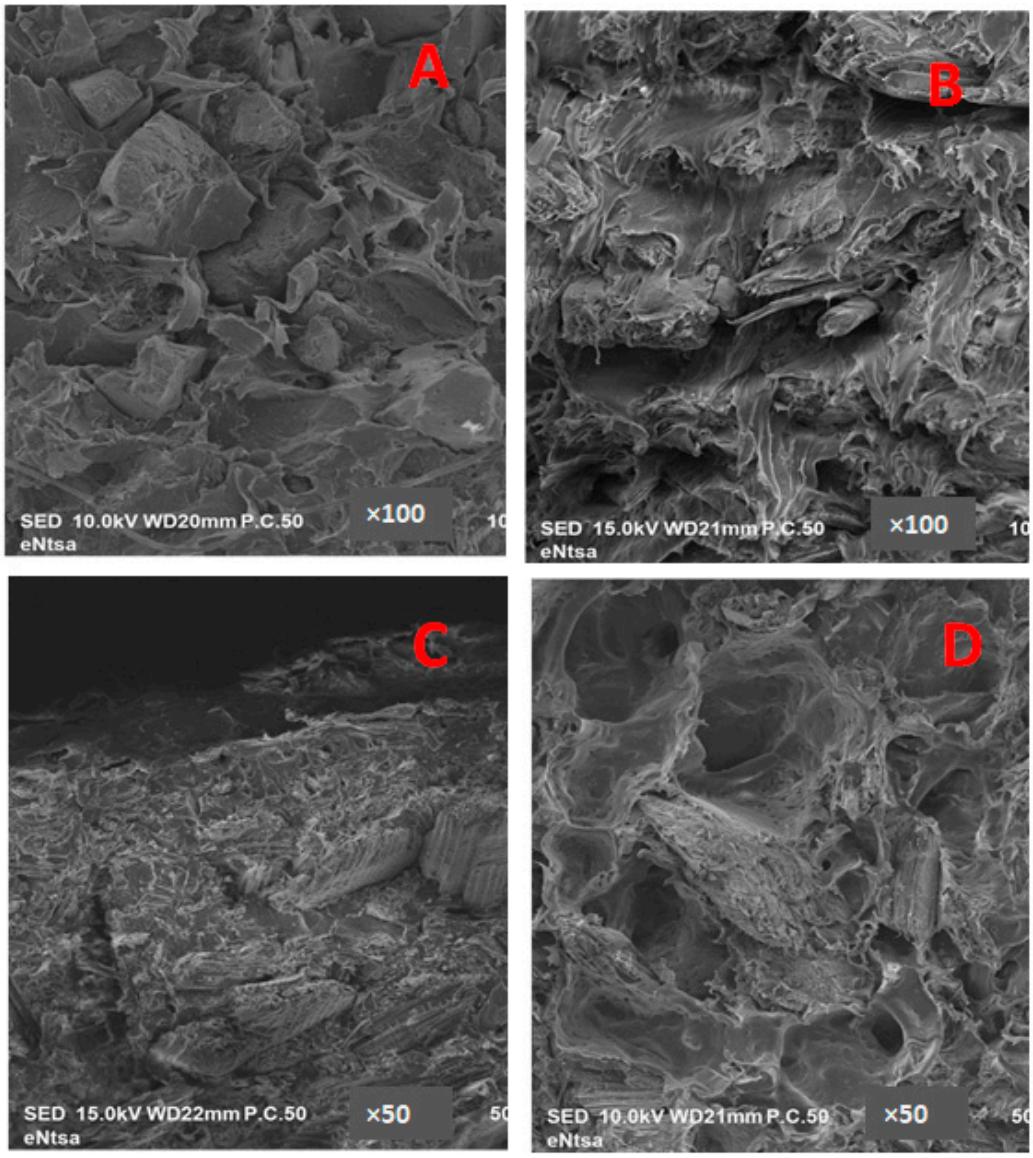

Figure 9. Scanning electron microscopy images of PP/GTR/WF composites with a magnification of 200 µm (**A**) Sample 1 with compatibilizer (**B**) Sample 2 with compatibilizer, (**C**) Sample 4 without compatibilizer, and (**D**) Sample 4 with compatibilizer.

The SEM image of the untreated ternary composite, Sample 4a, showed a hollow void, indicating that both fillers agglomerated in the middle part of the specimen, thus indicating that the agglomerated fillers detached from PP matrix. The SEM images of Sample 4b showed that PP is more compatible with WF than with GTR, since the WF particles were embedded in the PP matrix, as in Figure 9D. The GTR particles showed a weak interfacial adhesion and consequent detachment from the PP matrix, which resulted in several voids in the composites. The compatibilizer performed better with WF than GTR.

4. Conclusions

The statistically designed experiments using a simplex-centroid methodology approach was used to determine the proportions of PP, GTR, and WF required to determine the optimal properties of the binary and ternary composites. Several characterization and analytical techniques were employed to evaluate and compare proprieties of the blends relative to the neat PP. The addition of WF and GTR increased the glass transition temperature of the composites, and there was an increase in crystallization and melt temperature values

for both binary and ternary composites. The compatibilizer increased the thermal stability of composites comprising the largest amounts of PP and WF. The compatibilizer improved wetting amongst the components; TGA analysis showed that composites without compatibilizer displayed heterogeneous behaviour, but after the addition of the EB compatibilizer composites displayed homogeneity, therefore indicating that PP has encapsulated the WF particles. The incorporation of WF and GTR decreased the tensile strength of the composites. This might be due to poor interfacial adhesion among the components in the composites. Each filler can either have positive or negative effect, since the WF is hydrophilic and GTR is hydrophobic, hence, GTR could shield WF from absorbing water. The increase in GTR increased the elongation at break of the composites, and overall ternary composites showed better properties than binary ones. The storage modulus of the composites increases with the increased amount of the WF, due to the brittle and rigid nature of the fibre particles which disrupted the PP matrix. The incorporation of EB as a compatibilizer has reduced the stiffness of the composites, since it acted as a binder among the components.

The good wetting of composites that was achieved by the presence of compatibilizer decreased the water absorption, as the untreated composites showed a higher water uptake than the EB compatibilized composites. The composites with a higher quantity of WF absorbed water more than the composites with higher amounts of GTR. The morphology of various composites was also studied, and it was shown that PP was not compatible with both fillers, GTR and WF. However, the incorporation of a compatibilizer enhanced the interfacial adhesion between the PP matrix and filler particles, especially for the composites that contained a higher content of WF than GTR. The experimental mixture design showed that ternary composites have improved properties as compared to binary composites, and the use of more than one filler proved to provide balanced tensile and thermal stability properties of the composites.

Author Contributions: Conceptualization, S.P.H. and M.J.P.; methodology, L.M.; software, L.M. and M.J.P.; validation, L.M., M.J.P., K.G. and S.P.H.; formal analysis, L.M., M.J.P. and S.P.H.; investigation, L.M.; resources, S.P.H.; data curation, L.M., M.J.P., K.G. and S.P.H.; writing—original draft preparation, L.M. and M.J.P.; writing—review and editing, M.J.P., K.G. and S.P.H.; visualization, L.M., M.J.P., K.G. and S.P.H.; supervision, M.J.P., K.G. and S.P.H.; project administration, M.J.P. and S.P.H.; funding acquisition, S.P.H. All authors have read and agreed to the published version of the manuscript.

Funding: This research received no external funding.

Institutional Review Board Statement: Not applicable.

Informed Consent Statement: Not applicable.

Data Availability Statement: The data presented in this study are available on request from the corresponding author.

Acknowledgments: The authors would like to thank Nelson Mandela University for the financial support, and Carst & Walker Company (Pty) Ltd. for providing ethylene-1-butene for the present study.

Conflicts of Interest: The authors declare no conflict of interest.

References

1. Toommee, S.; Pratumpong, P. PEG-Template for Surface Modification of Zeolite: A Convenient Material to the Design of Polypropylene Based Composite for Packaging Films. *Results Phys.* **2018**, *9*, 71–77. [CrossRef]
2. Simon, D.Á.; Halász, I.Z.; Karger-Kocsis, J.; Bárány, T. Microwave Devulcanized Crumb Rubbers in Polypropylene Based Thermoplastic Dynamic Vulcanizates. *Polymers* **2018**, *10*, 767. [CrossRef] [PubMed]
3. Ndiaye, D.; Diop, B.; Thiandoume, C.; Fall, P.A.; Farota, K.A.; Tidjani, A. Morphology and Thermo Mechanical Properties of Wood/Polypropylene Composites. In *Polypropylene*; Intech Open Acess: London, UK, 2012; pp. 415–425. ISBN 978-953-51-0636-4.
4. Luo, J.; Li, Q.; Shang, H.; Gao, S.; Zhang, C.; Sun, S. Mechanical and Damping Properties of Wood Plastic Composite Modified by Ground Waste Rubber Tire. *Prog. Rubber. Plast. Recycl. Technol.* **2017**, *33*, 127–138. [CrossRef]
5. Song, Y.; Wang, Q.; Han, G.; Wang, H.; Gao, H. Effects of Two Modification Methods on the Mechanical Properties of Wood Flour/Recycled Plastic Blends Composites: Addition of Thermoplastic Elastomer SEBS-g-MAH and in-Situ Grafting MAH. *J. For. Res.* **2010**, *21*, 373–378. [CrossRef]
6. Soccalingame, L.; Perrin, D.; Bénézet, J.-C.; Bergeret, A. Reprocessing of UV-Weathered Wood Flour Reinforced Polypropylene Composites: Study of a Natural Outdoor Exposure. *Polym. Degrad. Stab.* **2016**, *133*, 389–398. [CrossRef]
7. Caveda, S.; Pérez, E.; Blázquez-Blázquez, E.; Peña, B.; van Grieken, R.; Suárez, I.; Benavente, R. Influence of Structure on the Properties of Polypropylene Copolymers and Terpolymers. *Polym. Test.* **2017**, *62*, 23–32. [CrossRef]
8. Maddah, H.A. Polypropylene as a Promising Plastic: A Review. *Am. J. Polym. Sci.* **2016**, *6*, 1–11. [CrossRef]
9. Girones, J.; Vo, L.T.T.; Haudin, J.-M.; Freire, L.; Navard, P. Crystallization of Polypropylene in the Presence of Biomass-Based Fillers of Different Compositions. *Polymer (Guildf).* **2017**, *127*, 220–231. [CrossRef]
10. Kazemi Najafi, S. Use of Recycled Plastics in Wood Plastic Composites—A Review. *Waste Manag.* **2013**, *33*, 1898–1905. [CrossRef]
11. Zhao, J.; Wang, X.-M.; Chang, J.M.; Yao, Y.; Cui, Q. Sound Insulation Property of Wood–Waste Tire Rubber Composite. *Compos. Sci. Technol.* **2010**, *70*, 2033–2038. [CrossRef]
12. Chan, C.M.; Vandi, L.-J.; Pratt, S.; Halley, P.; Richardson, D.; Werker, A.; Laycock, B. Composites of Wood and Biodegradable Thermoplastics: A Review. *Polym. Rev.* **2018**, *58*, 444–494. [CrossRef]
13. Ramarad, S.; Khalid, M.; Ratnam, C.T.; Chuah, A.L.; Rashmi, W. Waste Tire Rubber in Polymer Blends: A Review on the Evolution, Properties and Future. *Prog. Mater. Sci.* **2015**, *72*, 100–140. [CrossRef]
14. Peng, Y.; Liu, R.; Cao, J. Characterization of Surface Chemistry and Crystallization Behavior of Polypropylene Composites Reinforced with Wood Flour, Cellulose, and Lignin during Accelerated Weathering. *Appl. Surf. Sci.* **2015**, *332*, 253–259. [CrossRef]
15. Li, Y. Effect of Woody Biomass Surface Free Energy on the Mechanical Properties and Interface of Wood/Polypropylene Composites. *J. Adhes. Sci. Technol.* **2014**, *28*, 215–224. [CrossRef]
16. Yi, S.; Xu, S.; Fang, Y.; Wang, H.; Wang, Q. Effects of Matrix Modification on the Mechanical Properties of Wood–Polypropylene Composites. *Polymers* **2017**, *9*, 712. [CrossRef] [PubMed]
17. Ayyer, R.; Rosenmayer, T.; Schreiber, W.; Colton, J. Effects of Micronized Rubber Powders on Structure and Properties of Polypropylene Composites. *Waste Biomass Valorization* **2013**, *4*, 65–71. [CrossRef]
18. Zedler, Ł.; Colom, X.; Saeb, M.R.; Formela, K. Preparation and Characterization of Natural Rubber Composites Highly Filled with Brewers' Spent Grain/Ground Tire Rubber Hybrid Reinforcement. *Compos. Part B Eng.* **2018**, *145*, 182–188. [CrossRef]
19. Khan, M.Z.R.; Srivastava, S.K.; Gupta, M.K. A State-of-the-Art Review on Particulate Wood Polymer Composites: Processing, Properties and Applications. *Polym. Test.* **2020**, *89*, 106721. [CrossRef]
20. Monteiro, S.N.; Lopes, F.P.D.; Ferreira, A.S.; Nascimento, D.C.O. Natural-Fiber Polymer-Matrix Composites: Cheaper, Tougher, and Environmentally Friendly. *JOM* **2009**, *61*, 17–22. [CrossRef]
21. Shubhra, Q.T.H.; Alam, A.; Quaiyyum, M.A. Mechanical Properties of Polypropylene Composites: A Review. *J. Thermoplast. Compos. Mater.* **2011**, *26*, 362–391. [CrossRef]
22. Sienkiewicz, M.; Janik, H.; Borzędowska-Labuda, K.; Kucińska-Lipka, J. Environmentally Friendly Polymer-Rubber Composites Obtained from Waste Tyres: A Review. *J. Clean. Prod.* **2017**, *147*, 560–571. [CrossRef]
23. Zedler, Ł.; Burger, P.; Wang, S.; Formela, K. Ground Tire Rubber Modified by Ethylene-Vinyl Acetate Copolymer: Processing, Physico-Mechanical Properties, Volatile Organic Compounds Emission and Recycling Possibility. *Materials* **2020**, *13*, 4669. [CrossRef] [PubMed]
24. Das, S.C.; Ashek-E-Khoda, S.; Sayeed, M.A.; Suruzzaman; Paul, D.; Dhar, S.A.; Grammatikos, S.A. On the Use of Wood Charcoal Filler to Improve the Properties of Natural Fiber Reinforced Polymer Composites. *Mater. Today Proc.* **2021**, *44*, 926–929. [CrossRef]
25. Parenteau, T.; Ausias, G.; Grohens, Y.; Pilvin, P. Structure, Mechanical Properties and Modelling of Polypropylene for Different Degrees of Crystallinity. *Polymer* **2012**, *53*, 5873–5884. [CrossRef]
26. Hrdlicka, Z.; Kuta, A.; Hajek, J. Thermoplastic Elastomer Blends Based on Waste Rubber and Low-Density Polyethylene. *Polimery* **2010**, *55*, 832–838. [CrossRef]
27. Friedrich, D. Post-Process Hot-Pressing of Wood-Polymer Composites: Effects on Physical Properties. *J. Build. Eng.* **2022**, *46*, 103818. [CrossRef]
28. Petchwattana, N.; Covavisaruch, S. Mechanical and Morphological Properties of Wood Plastic Biocomposites Prepared from Toughened Poly(Lactic Acid) and Rubber Wood Sawdust (Hevea Brasiliensis). *J. Bionic Eng.* **2014**, *11*, 630–637. [CrossRef]
29. Phiri, M.J.; Phiri, M.M.; Mpitso, K.; Hlangothi, S.P. Curing, Thermal and Mechanical Properties of Waste Tyre Derived Reclaimed Rubber–Wood Flour Composites. *Mater. Today Commun.* **2020**, *25*, 101204. [CrossRef]

30. Guo, D.; Guo, N.; Fu, F.; Yang, S.; Li, G.; Chu, F. Preparation and Mechanical Failure Analysis of Wood-Epoxy Polymer Composites with Excellent Mechanical Performances. *Compos. Part B Eng.* **2022**, *235*, 109748. [CrossRef]
31. Ciro, E.; Parra, J.; Zapata, M.; Murillo, E.A. Effect of the Recycled Rubber on the Properties of Recycled Rubber/Recycled Polypropylene Blends. *Ngeniería Y Cienc.* **2015**, *11*, 173–188. [CrossRef]
32. Fan, Y.; Mei, C.; Liu, Y.; Mei, L. Effect of Surface Free Energy of Wood-Flour and Its Polar Component on the Mechanical and Physical Properties of Wood-Thermoplastic Composites. *Rev. Adv. Mater. Sci.* **2013**, *33*, 211–218.
33. De, D.; Panda, P.K.; Roy, M.; Bhunia, S. Reinforcing effect of reclaim rubber on natural rubber/polybutadiene rubber blends. *Mater. Des.* **2013**, *46*, 142–150. [CrossRef]
34. Joseph, S.; Appukuttan, S.P.; Kenny, J.M.; Puglia, D.; Thomas, S.; Joseph, K. Dynamic mechanical properties of oil palm microfibril-reinforced natural rubber composites. *J. Appl. Polym. Sci.* **2010**, *117*, 1298–1308. [CrossRef]